

Interline Unified Power Quality Conditioner for Enhancing Power Quality using FOFPID-based Interleaved CUK Converter

*^{1,2}Rajakumar P, ³Dr. R. Saravanakumar

¹Research Scholar, School of Electrical Engineering,

Vellore Institute of Technology, Vellore, Tamil Nadu 632014, India.

²Associate Professor, Department of Electrical and Electronics Engineering,

Sri Sairam Engineering College, Chennai – 600 044, Tamil Nadu, India.

*Email: rajakumar.eee@sairam.edu.in

³Professor, School of Electrical Engineering,

Vellore Institute of Technology, Vellore, Tamil Nadu 632014, India.

Email: rsaravanakumar@vit.ac.in

Abstract: Electrical distribution systems face increased non-linear loads due to using power electronics for the converters. Due to these non-linear loads, the system exhibits PQ problems in the distributed feeders. To enhance PQ problems in the dual feeder, fractional order fuzzy proportional integral derivative controller (FOFPID) is introduced with interline unified power quality (IUPQC) conditioner. IUPQC conditioner includes a distribution static compensator (DSTATCOM), dynamic voltage restorer (DVR) and interleaved cuk converter (ICC). DSTATCOM and DVR are used for compensating the voltages and current in the dual feeders (feeder-1 and feeder-2). Also, ICC monitors the switching between the DSTATCOM and DVR compensators by providing proper power flow. Moreover, the FOFPID controller regulates an input supply from both feeders. The simulation is performed through MATLAB/Simulink platform, demonstrating the robustness of a proposed FOFPID with an IUPQC controller. The performance of a proposed controller is analyzed through two cases for both feeders. Furthermore, the total harmonic distortions (THD) are calculated for the feeder parameters. The proposed FOFPID with IUPQC controller also maintains stability in a dual feeder. Therefore, the entire response shows the functionality and feasibility of a proposed controller.

Keywords: power quality, distribution static compensator, dynamic voltage restorer, interline unified power quality conditioner, dual feeder, interleaved cuk converter, total harmonic distortion.

I. INTRODUCTION

Power quality (PQ) must be maintained at a predetermined standard level for non-linear load in distributed generator networks. Over 90% of PQ events like voltage sagging, swelling, and transitory disruptions significantly influence sensitive loaded conditions [1]. With other failures, switching of massive parallel capacitors, transformer stimulating, and activating rotating machines are the main causes of voltage sag [2]. Many power electronics-based alternatives have already been proposed to address the PQ troubles in dual feeders [3]. The distribution system with renewable sources is emerging in relevance due to economic issues and growing environmental awareness [4]. Renewable energy sources like wind, solar, biomass and fuel cell are introduced with the power system for enhancing PQ troubles [5]. Some of the techniques include the usage of fault current compensators (FCC), dynamic voltage restorers (DVR), solid-state transfer switches (SSTS), Distribution static compensators (DSTATCOM), static VAR compensators and unified PQ controllers (UPQC). DVR performs the operating function by injecting the compensation

voltage in series with the vulnerable electrical transmission feeder [6-7]. This transmission feeder operates with appropriate amplitude, phase difference and frequencies. Several DVRs have been presented with various topologies, operational strategies and battery packs [8]. The main drawback of DVR is that its DC-link capacitor is substantially larger and more expensive. Moreover, DVR requires higher active power (AP) to make phase difference adjustments in voltage [9].

A novel control strategy is suggested for reducing the AP contribution of DVR rather than raising the capacity of DVR. The failures in most unprotected external feeders are successfully rectified using FCC at the beginning of a feeder [10]. Similarly, DSTATCOM devices are also used to support voltage interruptions in sensitive loads. Even though DSTATCOM controls the transient characteristics of voltage, it does not enhance the AP [11]. For resolving the PQ troubles in dual feeder construction, UPQC is also utilized with compensators. UPQC enhances reactive power (RP) and AP with large DC-link capacitors. UPQC also provides excellent system performance for compensating power flow in dual

feeders [12]. The optimization approaches are also exhibited with the controllers for improving the performance of a power system [13]. The climatic changes in the environment cause changes in the renewable source, affecting the power flow in the distributed system [14]. For maintaining the controlled voltage over the system, the controllers like proportional-integral (PI) controllers are also introduced [15]. While constructing the dual feeders, the link converter is necessary for regulating the voltages between the feeders. Therefore, the PQ troubles are reduced using the appropriate compensator to maintain the stability of the power system.

The following terms provide the main goals of this paper:

- A fractional order fuzzy proportional integral derivative (FOFPID) controller is introduced to maintain the dual feeders' stability.
- A distribution static compensator (DSTATCOM) is suggested to compensate for the PQ issues in feeder-1.
- Dynamic voltage restorer (DVR) is developed for improving PQ events in feeder-2.
- DVR and DSTATCOM are linked with the interleaved cuk converter (ICC) to regulate the voltage between the feeders.

The rest of the paper is structured as follows: Section 2 reveals the works on PQ enhancement in dual feeders. Section 3 describes the proposed methodology, and Section 4 signifies the observed results. Also, Section 5 concludes the paper with future work.

II. RELATED WORKS

Various controllers compensate for feeders' PQ troubles; some controller strategies are discussed here.

Das et al. [16] developed a fuzzy logic controller (FLC) for enhancing PQ troubles in hybrid renewable (solar, wind and fuel cell) power systems. The interruptions in a common coupling point (CCP) were rectified by the fuel cell, which serves as the controller in a hybrid system. Moreover, the developed FLC detects and rectifies the source current signal distortions. The harmonics in the load-side current have been minimized by injecting the compensating current into the source current. The developed FLC controller was more suitable for non-linear and linear loads. The main advantage of FLC was that the execution time was fast with less intricacy. The minimum total harmonic distortion (THD) was also evaluated for both loaded conditions with better efficiency.

Abas et al. [17] introduced the DVR for improving PQ events in a distributed system with non-linear loads (NLL). The system performance was analyzed by injecting the faults on a source side. The distorted supply includes 3rd and 5th-order harmonics, and DVR regulated the harmonics with control methodologies. Due to the enhanced performance of DVR, the generated load voltage was effectively smooth with minimum

disruptions. The characteristic response was analyzed through various cases to verify the robustness of DVR. Besides, THD for the voltage at load was reduced from 18% to 4%. Therefore, DVR effectively operates on different loaded conditions and compensates PQ in a distributed system.

Naidu et al. [18] evolved the distributed power flow controller (DPFC) with fractional order proportional integral derivative (FOPID) controller and PQ concept for compensating PQ. The wind and solar power sources were considered the source power generating system. FOPID controller compensates the supply voltage by raising the peak amplitude when the sag fault occurs. Similarly, FOPID drops the amplitude of a source voltage when the generated voltage is swelled. Therefore, FOPID competently reduces the distortions using parallel and series filters in the DPTC compensator. The output response reveals the behaviour of DPTC, and the comparative analysis signifies the functionality of DPTC.

Goud et al. [19] examined the PQ troubles in the distributed power system by introducing the black widow optimization algorithm (BWOA) with the FOPID controller. Besides, DPTC was also suggested with FOPID for compensating PQ troubles in a hybrid power system. The wind and solar power system generates the power to satisfy the demand side response. Whether the generated power was insufficient to fulfil the load response, DPTC delivers sufficient power. BWOA-optimized FOPID enhances the PQ troubles by injecting the voltage and current into the unregulated power supply. The improved voltage was delivered to the load with fewer oscillations, and the results were analyzed for various loads.

Muthuvel et al. [20] suggested a quasi-Z-source inverter (QZI) with UPQC for the PQ problems in the solar-connected distributed system. Two filters were incorporated with UPQC to regulate the source's distorted voltage and current. The main goal of QZI was to convert the direct current (DC) supply to alternating current (AC) by minimizing the interruptions in a system. Also, UPQC plays an important role in the system for regulating the optimum voltage and current. The regulated supply is provided to the QZI through an enhanced 2nd order generalized integrator (E2OGI). Therefore, UPQC optimized E2OGI integrator satisfies the demand response by compensating for the solar-generated voltage.

Prakash et al. [21] introduced the IUPQC condition for restoring current and voltage to improve the PQ in different feeder-connected systems. The system includes 4 converters and space vector pulse width modulation (SVPWM) to minimize the difficulties in generated signals. The converters were concerned with the system with hexagonal coordinate axis components. Also, the feeders were linked through the common coupling capacitor to maintain proper transmission between the feeders. The suggested conditioner enhances the PQ troubles in

feeders with high distortions. This tends to be the main drawback in IUPQC with 4 converters.

Golla et al. [22] examined that a universal active power filter (UAPF) compensated for the PQ troubles in grid-connected renewable systems. The storage system was integrated with the hybrid wind and solar system along with the coupling capacitor. Microgrid controller (MGC) was developed with UAPF to compensate for the PQ troubles in the grid-connected system. The power balance strategy regulates the power transformation between the filters used in the system. Therefore, MGC monitors the generated signal from a hybrid renewable source, and UAPF enhances the PQ in a distributed system. The main demerits were that the compensation was not better during enhancing PQ.

A. Gowrishankarand M. Ramasamy [23] introduced UPQC conditioners based on the power angle control strategy (PAC) to enhance troubles in grid-connected renewable systems. The internal filters in UPQC compensate for voltage and current characteristics based on PAC. The PAC-UPQC conditioner increases the RP to minimize the distortions in power generated by renewable sources. PAC-UPQC operates based on the synchronous reference frame (SRF) approach for regulating the generated source. The behaviour of an introduced PAC-UPQC controller was examined through various faulty conditions such as variation in load, irradiance variation, sag and swell. The literature review shows that the controllers enhance the PQ troubles in the feeders with high distortions. Hence to overcome this drawback, the novel controller with ICC is introduced.

III. PROPOSED METHODOLOGY

Controlled and enhanced PQ is essential for the best resource exploitation in any electricity-powered sector. However, certain major issues with PQ have been identified, including interruptions, swelling, sagging, transient and harmonic distortions. To solve these issues, the novel IUPQC is introduced to enhance the PQ issues between two feeders in the distribution system. Feeder-1 and feeder-2 are the two feeders in which feeder-1 is connected to the electric arc furnace (EAF), and feeder-2 is connected to the non-linear load. The input for feeder-2 is from hybrid renewable sources such as tidal and wind, whereas the input for feeder-1 is an AC voltage source. FOFPID is introduced to regulate the source voltages from both feeders. Moreover, the DSTATCOM and DVR are proposed for enhancing PQ troubles in dual feeders. DVR and DSTATCOM devices are connected with ICC through the common coupling capacitor. ICC regulates the power flow between two feeders through DSTATCOM and DVR compensators. Therefore, the regulated supply from the FOFPID controller is compensated by DSTATCOM and DVR to enhance the PQ issues in feeders. The main objective of a proposed IUPQC is to enhance the PQ issues, regulate the voltage supply and maintain stability in the

feeders. Figure 1 illustrates the proposed methodology for improving PQ troubles in dual feeders.

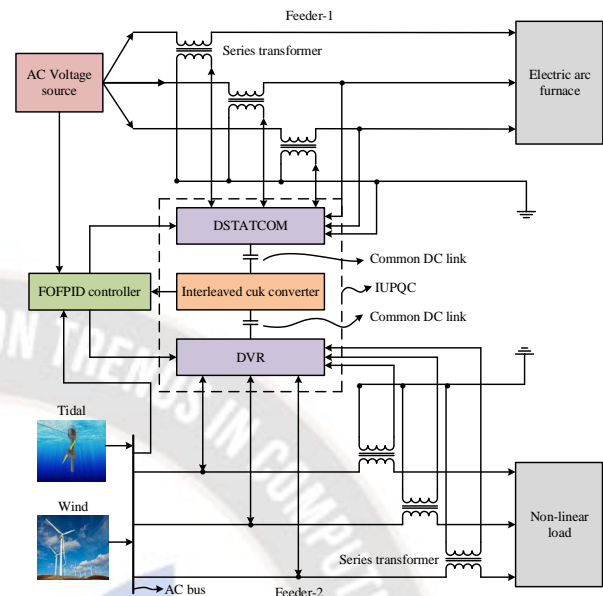


Figure 1: Proposed strategy for enhancing PQ in dual feeders

A. Modeling of tidal and wind system

The input source for feeder-2 is from the hybrid renewable source such as wind and tidal systems. The hybrid source requires the modelling equations for power generation, and the mathematical modelling is discussed here.

1 Tidal system:

The rise and fall of tides generate tidal energy due to an interrelationship between the sun and the earth. The rotational speed of a blade interrupts the upstream, and the downstream is highly disturbed when it is close to the turbine. Due to these characteristics, the torque is induced in the rotor, and the shaft connects rotor with the power generating system. The generated power is evaluated by using the basic equation,

$$J_t \frac{d\omega}{dt} = T_r - T_{mt} - \beta \omega \quad (1)$$

Where, J_t indicates the inertia of a rotor within the turbine ($\text{kg}\cdot\text{m}^2$), T_r is the electro-magnetic torque (N-m), T_{mt} is the mechanical torque in a rotor (N-m), β is the friction coefficient and ω is an angular speed of the rotor [24]. Therefore, the tidal turbine system generates power based on modelling characteristics.

2 Wind system:

The power generated by a wind turbine system characterizes the modelling of a wind turbine system. The input to a turbine

system is signified as wind velocity, and the power generated by the wind source is represented as mechanical power. The generated power is mathematically modelled as follows;

$$P_w = \frac{1}{2} \rho_d A_w V_w^3 \quad (2)$$

Here, P_w is the total power generated by a wind power plant, ρ_d represents the density of air (kg/m^3), A_w indicates the total area in a turbine and V_w refers to the velocity of wind (m/sec). The total power generated by the wind turbine system based on the probability of wind velocity is exhibited as;

$$P_{vw} = \begin{cases} P_a \frac{V_{vw}^2 - V_{sw}^2}{V_{wr}^2 - V_{sw}^2}; & V_{sw} < V_{wr} < V_{vw} \\ P_a ; & V_{wr} < V_{vw} < V_{sc} \\ 0 ; & V_{vw} \leq V_{sw} \text{ and } V_{vw} \geq V_{sc} \end{cases} \quad (3)$$

Where, P_a is the actual power in a system (W), V_{vw} is the velocity of wind (m/sec), V_{sw} is the cut-in speed of a wind (m/sec), V_{wr} is the rated speed of a wind (m/sec) and V_{sc} is the cut-off speed of a wind (m/sec). Therefore, the power generated from the wind turbine system is demonstrated based on the mathematical model [25].

B. Non-linear loads (NLL)

Every utility globally uses non-linear power devices, which rely on electrically powered switches for residential and commercial purposes. The NLL, such as drives with varying frequencies, furnaces and personal computers, exhibits the PQ issues such as noise, harmonic fluctuation and voltage distortion. These harmonic troubles generate heat in an electrical device, losses, system defects and packing faults [26]. Hence, the PQ compensation is essential for the NLL and is achieved using the compensators or controllers.

C. Modeling of an AC voltage source

An AC voltage source is the input to feeder-1, and the EAF is connected to the output side of feeder-1. AC voltage source signifies the source voltage, which preserves the sinusoidal voltage across the terminals on the output side. Also, the AC source voltage not depends on the terminal current flowing through the feeder. The AC source is in three phases and modelled with the series impedance. The output voltage from the AC voltage source is mathematically modelled as follows;

$$V_{ac} = V_{vo} \sin(2\pi \cdot f_a \cdot t + \lambda) \quad (4)$$

Where, V_{vo} represents the highest amplitude, and it is usually 1, f_a is the frequency and t refers to the time at which the voltage is measured. Also, the variable λ indicates the phase shift, which is assumed to be 0. Therefore, the AC source voltage is generated for the feeder-1 to deliver the power to EAF [27].

D. Designing of electric arc furnace (EAF)

The EAF is designed for a furnace's current and voltage characteristics at the output of feeder-1. The mathematical model equation describes the approximate voltage and current within the furnace. The arc length of EAF is recognized based on two parameters: destruction and agitating voltage. Various methodologies like piecewise strategy, approximation strategy and hybrid of hyperbolic and exponential strategy are used for examining the characteristics of EAF. While comparing these methodologies, the approximation strategy is used for extracting the voltage and current behaviour of EAF. During the function of EAF, the arc length is determined for evaluating the agitating and destruction voltage. The voltage behaviour is analyzed based on the equation;

$$V = \begin{cases} S_a i, & i \leq i_a \\ S_b i + V_i \left(1 - \frac{S_b}{S_a}\right), & i \leq i_b \\ S_b i - V_i \left(1 - \frac{S_b}{S_a}\right), & -i_b \leq i \leq -i_a \end{cases} \quad (5)$$

Where, S_a and S_b are the slopes between the actual and modelled characteristics. Also, V_i indicates the agitating voltage for the arc currents. Here, i_b and i_a are the arc current for agitating voltage and destruction voltage, respectively. The arc current due to the agitating voltage is given by,

$$i_a = \frac{V_i}{S_a} \quad (6)$$

Furthermore, the arc current due to the destruction voltage is evaluated based on the equation,

$$i_b = \frac{V_d}{S_b} - V_i \left(\frac{1}{S_b} - \frac{1}{S_a} \right) \quad (7)$$

The arc voltage is characterized by analyzing arc current in EAF, and the equation which relates arc current and arc voltage is given by;

$$V_{arc} = V_t \times \left(1 - e^{\frac{i}{i_q}} \right) \quad (8)$$

Where, V_{arc} signifies the arc voltage, V_t refers to the optimum voltage, i refers to the arc current in a single phase and i_q is the fixed current value (either negative or positive). Therefore, the EAF is modelled based on the arc length, and the corresponding current-voltage behaviour is determined [28]. The input signal and the output from the DSTATCOM compensator are given to each phase of EAF. The regulated voltage from the compensator is given to the EAF load.

E. Modeling of IUPQC conditioner

Due to high switching loss in UPQC, IUPQC is proposed for compensating PQ problems in dual feeder networks. Maintaining the switching frequency at a minimum is essential to increase the device's rating potential in the network. The DSTATCOM compensator, DVR and ICC are combined to form an IUPQC conditioner. DSTATCOM is one of the voltage source converters (VSC) used to regulate system voltage to enhance reactive power. For enhancing the PQ events in the distributed feeder networks, DVR is introduced. DVR compensates for the voltage sag and voltage swell in the generated source voltage. ICC is one of the DC-DC converters which deliver the output voltage with higher or lower amplitude than the input voltage. ICC is constructed with a buck converter, boost converter and coupling capacitor. The buck-boost converter generates a reversed output with a discontinuous capacitor current, leading to some defects. Due to this drawback, ICC is used for monitoring the switching between DSTATCOM and DVR. The main advantage of ICC is that it maintains a continuous current flow in the dual-feeder system. Therefore, IUPQC injects the compensated voltage and current into the input voltage to rectify the distortions.

DSTATCOM reduces the PQ troubles in the device connected in parallel with the feeder system. The voltage levels are rectified during the system's faulty conditions using DSTATCOM. Usually, DSTATCOM is designed based on a voltage source converter (VSC) with IGBT switches. DSTATCOM is more suitable for compensating PQ problems under various loaded conditions. But, the drawback is that DSTATCOM doesn't operate properly in a low-impedance system. If the input voltage amplitude exceeds the system voltage, the current flows from the converter to a system. Thus, the converter generates the RP, which is capacitive. Similarly, if the input voltage amplitude is lower than the device voltage, the current flows from the system to a converter. This process is inductive, and the converter consumes RP. The primary

purpose of DVR is to safeguard delicate loads against PQ problems, including voltage swell and voltage sag. The PQ troubles are compensated by injecting the voltage across the feeders.

1 Modeling of ICC

The main goal of ICC is to convert the voltage from input side to the output side with opposite polarity. ICC enhances the power flow on both sides by minimizing the current ripples in the system. The architecture of ICC consists of two diodes (d_1 , d_2) and two switches (S_{w1} , S_{w2}) with a larger frequency rate. Moreover, ICC includes four capacitors (C_1 , C_2 , C_3 and C_4) and four inductors (L_1 , L_2 , L_3 and L_4) along with the resistance at a load side.

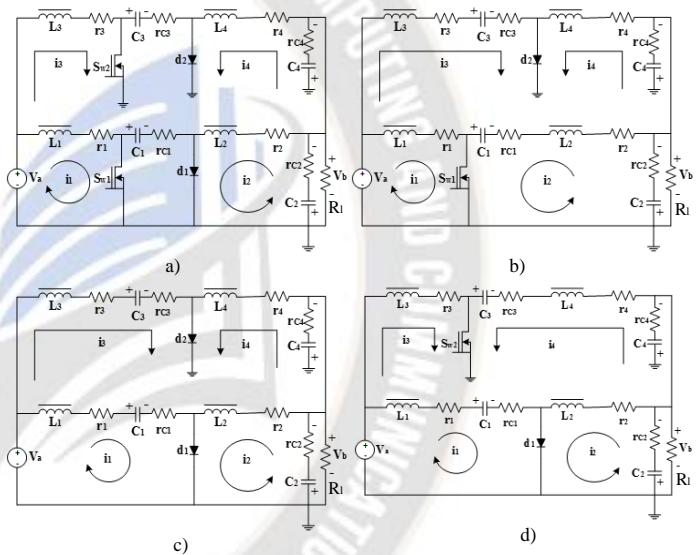


Figure 2: a) Basic circuit model of ICC, b) Schematic representation of ICC for condition 1, c) Schematic representation of ICC for condition 2 and d) Schematic representation of ICC for condition 3

The functional characteristics of ICC are analyzed through four basic conditions based on the phase shift pulse width modulation (PSPWM) strategy. An optimum range for the duty ratio is nearly 50%, so the current ripple is also minimized to 50%. The basic four conditions are listed below.

- ❖ Condition 1: S_{w1} is ON and S_{w2} is OFF
- ❖ Condition 2: S_{w1} is OFF and S_{w2} is OFF
- ❖ Condition 3: S_{w1} is OFF and S_{w2} is ON

The basic circuit model of ICC includes 4 blocks with inductors, capacitors, diodes, switches and their respective

resistive components. Figure 2 (a) shows the circuit model of ICC. Table 1 reveals the operational characteristics of ICC.

Table 1: Operational characteristics of ICC

Conditions	S_{w1}	S_{w2}	d_1	d_2	Output
Condition-1	On	Off	Off	On	C_1 \rightarrow Load
Condition-2	Off	Off	On	On	L_2, L_4 \rightarrow Load
Condition-3	Off	On	On	Off	C_1 \rightarrow Load

Condition 1: When the switch S_{w1} is in ON condition and the switch S_{w2} is in OFF condition, then the inductor L_1 gets charged, and the inductor L_2 gets discharged. Moreover, the energy stored in the inductor L_3 is transferred to the capacitor C_3 . Further, the capacitor C_1 discharges and the energy is delivered to the load. The load current is fixed to remain constant, and the polarity is assumed to be negative. Therefore, due to the charging of an inductor L_1 , the reduction in current ripple is given by;

$$\Delta I_{L1} = \left(\frac{(T_1 - T_0)}{L_1} \right) (V_a - r_1 i_{L1}) \quad (9)$$

$$\Delta I_{L3} = \left(\frac{(T_1 - T_0)}{L_3} \right) (V_a - V_{C3} - (r_3 + r_{C3}) i_{L3}) \quad (10)$$

Here, V_a indicates the input voltage, R_l refers to the load resistance and V_b signifies the output voltage. Consider, $L_1 = L_3 = L_m$, $r_1 = r_3$, $i_{L1} = i_{L3}$ then the transformed equation is expressed as,

$$\Delta I_1 = \Delta I_{L1} - \Delta I_{L3} = (V_{C3} + r_{C3} * i_{L3}) \left(\frac{(T_1 - T_0)}{L_m} \right) \quad (11)$$

Here, T_1 and T_0 indicates the time duration, the circuit diagram in Figure 2(b) signifies the components corresponding to condition 1. Figure 2 (b) depicts that the switch S_{w2} and the diode d_1 are in OFF condition. Therefore, the characteristic response corresponding to condition 1 is determined based on the current flow in ICC.

Condition 2: In ICC, both switches S_{w1} and S_{w2} are assumed to be in OFF condition for the given time. In this mode

of operation, both inductors L_1 and L_3 discharges the energy and deliver it to the capacitors. The capacitors C_1 and C_3 consumes power and operate for a given time. Simultaneously, the inductors L_2 and L_4 discharges the energy and transfer the energy to a load side. Similarly, ICC transfers the power from DSTATCOM to DVR and vice versa. Due to the discharging in inductors, the current ripple generates, and it is expressed as,

$$\Delta I_{L1} = \left(\frac{(T_2 - T_1)}{L_1} \right) (V_a - V_{C1} - (r_1 + r_{C1}) i_{L1}) \quad (12)$$

$$\Delta I_{L3} = \left(\frac{(T_2 - T_1)}{L_3} \right) (V_a - V_{C3} - (r_3 + r_{C3}) i_{L3}) \quad (13)$$

By assuming, $L_1 = L_3$, $r_1 = r_3$, $V_{C1} = V_{C3}$ and $r_{C1} = r_{C3}$ then the transferred current by ICC is evaluated as,

$$\Delta I_2 = \Delta I_{L1} - \Delta I_{L3} = 0 \quad (14)$$

Therefore, the transformation of energy between the compensators is regulated by the ICC converter for time. Figure 2 (c) shows the model diagram of ICC for condition 2.

Condition 3: ICC converter delivers the power to a load by compensating the source voltage with such conditions. In condition 3, the switch S_{w1} is OFF, and the switch S_{w2} is ON over the time interval between T_2 and T_3 . During this mode, the inductor L_3 gets charged, and the inductor L_1 gets discharged. The energy from L_1 transferred to the capacitor C_1 , and the capacitor C_3 gets discharged. Hence, the energy stored in the capacitor C_1 is delivered to the corresponding feeder. The current ripple for condition 3 is demonstrated as follows;

$$\Delta I_{L1} = \left(\frac{(T_3 - T_2)}{L_1} \right) (V_a - V_{C1} - (r_1 + r_{C1}) i_{L1}) \quad (15)$$

$$\Delta I_{L3} = \left(\frac{(T_3 - T_2)}{L_3} \right) (V_a - r_3 \cdot i_{L3}) \quad (16)$$

By considering, $L_1 = L_3 = L_m$, $r_1 = r_3$ and $i_{L1} = i_{L3}$ then the delivered energy to a feeder is exhibited based on the equation;

$$\Delta I_3 = \Delta I_{L1} - \Delta I_{L3} = (-V_{C1} - r_{C1} * i_{L1}) \left(\frac{(T_3 - T_2)}{L_m} \right) \quad (17)$$

Hence, the ICC converter transfers the power or energy between the dual feeders for the compensators. Figure 2 (d) describes the power flow characteristics for condition 3.

The overall response from the ICC converter is evaluated based on the capacitor's characteristics C_1 . When the capacitor C_1 is assumed as the source, the voltage across the loops (V_{L1} , V_{L2}) tends to be zero. Then, the corresponding voltage across ICC is determined as;

$$V_{C1} = V_a + V_{C2} \quad (18)$$

Where, V_{C1} is the voltage across the capacitor C_1 and V_{C2} represents the voltage across the capacitor C_2 . The switching characteristics in a switch S_{w1} is examined based on the equation,

$$V_a D t_s / 2 + (V_a - V_{C1})(1 - D)t_s / 2 = 0 \quad (19)$$

Here, t_s refers to the switching duration of time and

$$D = \left(\frac{T_{ON}}{t_s / 2} \right). \text{ Also, } T_{ON} \text{ means the time at which the}$$

switch S_{w1} is in ON condition. The voltage across the capacitor C_2 is demonstrated by using the equation;

$$V_{C2} = -\frac{V_a D}{(1 - D)} \quad (20)$$

By analyzing all these conditions, it is clear that the ICC converter can handle the voltage across the compensators [29]. Table 2 describes the design values for the components in ICC.

Table 2: Designing parameter values for ICC

Parameters	Values
Input voltage (V_a)	20V
Output voltage (V_b)	-15V
L_1 and L_3	0.75mH
L_2 and L_4	0.1mH
C_1 and C_3	10 μ F
C_2 and C_4	22 μ F
R_l	7.5 Ω

Thus, the switching characteristics of DSTATCOM and DVR are determined effectively based on the components in the ICC architecture. Thus, the controller and the compensators regulate the voltage from the source. This rectified voltage is

delivered to the feeders, and the corresponding response is analyzed.

F. Modeling of FOFPID controller

The performance of a system is improved by using the traditional fuzzy inference system, which also offers more flexibility while tuning the additional parameters. The source voltage from both feeders is regulated using the suggested FOFPID controller and maintains stability in the feeder system. FOFPID controller regulates the AC source voltage from feeder-1 and feeder-2 and delivers the regulated voltage to DSTATCOM and DVR. The transfer function of the FOFPID controller is expressed as follows;

$$U_{FOFPID}(t) = S_q \cdot U_{FL}(t) + S_p \cdot \frac{d^{-\mu} U_{FL}(t)}{dt^{-\mu}} \quad (21)$$

$$U_{FL}(t) = F \left(S_n e(t), S_{mn} \cdot \frac{d^\lambda e(t)}{dt^\lambda} \right) \quad (22)$$

Where, $U_{FOFPID}(t)$ refers to the transfer function of a FOFPID controller, $e(t)$ represents the error function and λ is the fractional derivative order constant. Also, μ is the fractional integrative order constant, $U_{FL}(t)$ signifies an output from the fuzzy logic controller and $\frac{d^\lambda}{dt^\lambda}$ implies the differential function. Moreover, $\frac{d^{-\mu}}{dt^{-\mu}}$ indicates the integral function, S_q and S_p are the scaling components at the output side. Figure 3 describes the architecture of a FOFPID controller.

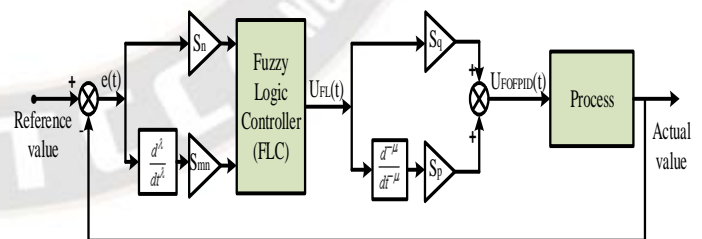


Figure 3: Architecture of FOFPID controller

S_n and S_{mn} are the scaling components of error value and derivative error value at the input side. The variable F represents the non-linear function factor which performs the function of mapping output and input components in a fuzzy controller. The fuzzy controller delivers the output based on the fuzzy rules and generates the membership function (MF) for each input component [30]. While enhancing PQ, FOFPID

reduces more oscillations than the other controllers. Therefore the proposed FOPID controller generates the regulated voltage based on the tuning parameters such as S_q , S_p , S_n and S_{mn}

IV. RESULT AND DISCUSSION

The enhancement of PQ in dual feeders based on IUPQC with FOPID controller is determined, and the obtained results are discussed here. The source voltage for feeder-1 and feeder-2 is assumed as 11kV. The simulation is performed through MATLAB/Simulink, and the performance shows the robustness of a proposed controller. The characteristics response of DSTATCOM and DVR is analyzed for various faulty conditions. Moreover, the THD is also examined for all voltage and current parameters in both feeders. The THD response is compared with existing IUPQC with a 4 voltage source converter (IUPQC-4VSC) [21]. The performance of the proposed controller is analyzed through different cases. Table 3 signifies the characteristics of system parameters.

Table 3: Specifications for system parameters

Parameters	Value
System frequency	50 Hz
Source voltage (feeder-1)	11 kV
Source voltage (feeder-2)	11kV
Rated current (feeder-1)	150A
Rated current (feeder-2)	150A
Feeder-1	$6.05 + j 36.28 \Omega$
Feeder-2	$3.05 + j 18.14 \Omega$
NLL	$250 + j 31.42 \Omega$
EAF	Phase 1: $24.2 + j 60.50 \Omega$ Phase 2: $36.2 + j 78.54 \Omega$ Phase 3: $48.2 + j 94.25 \Omega$

A. Characteristics response of the renewable source

In feeder-2, the source voltage is generated by hybrid renewable sources such as tidal and wind sources. The optimum range of tidal power is assumed to be 3kW, and the wind's rated power is 8kW. The FOPID controller and DVR compensator regulate the generated power from the renewable source. The characteristic values for wind and tidal turbine systems are tabulated in Table 4.

Table 4: Characteristics of wind and tidal turbine system

Parameter	Wind parameter	Values
Wind	Rated speed (m/sec)	10.5
	Rated power (KW)	8
	Number of blades	3
	Rotor diameter (m)	6.7
	Rated voltage (V)	220
Tidal	Rated power (kW)	3
	Cut-in speed (m/sec)	1.5
	Cut-off speed (m/sec)	5
	Rated voltage (V)	200
	Rated speed (rpm)	2500

Figure 4 (a) reveals the characteristic response of tidal power, and Figure 4 (b) depicts the performance of wind power. The generated power is sufficient to satisfy the demand side response. The NLL is connected to feeder-2 through DVR and the series transformer. The compensators rectify faults in a generated voltage and deliver to the load. The time duration for analyzing tidal and wind performance is assumed to be 1 second.

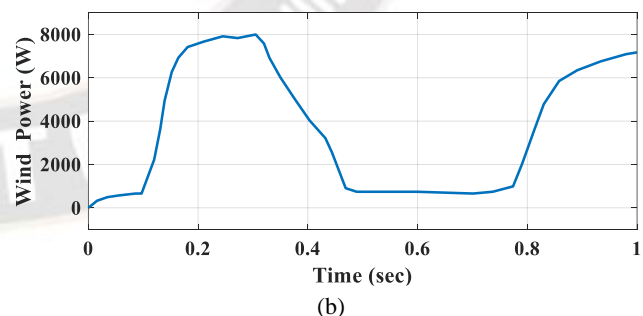
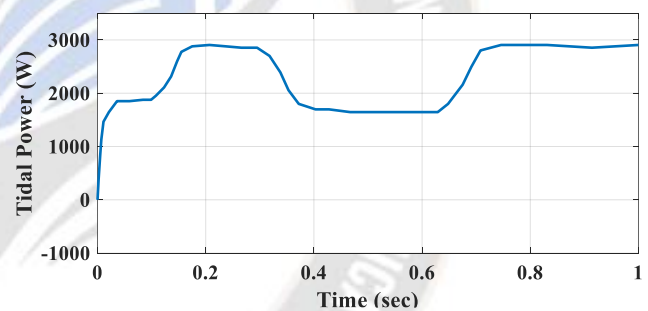


Figure 4: Simulation response of (a) tidal power and (b) wind power

B. Simulation response of feeder-1 for proposed IUPQC with FOPID controller

The three-phase AC voltage source is applied to the feeder-1, and a proposed IUPQC with the FOPID controller rectifies the faults in a source voltage. The performance of a proposed IUPQC with a FOPID controller is demonstrated through two

faults. For feeder-1, the detection and compensation of voltage and current sagging are exhibited.

The source side voltage for feeder-1 is initialized as 11kV, and the respective performance on the load side is analyzed through the DSTATCOM compensator. The voltage at source side is determined as defective, and the FOFPID controller regulates the defects. The regulated voltage is given to the DSTATCOM compensator for injecting the defective voltage amplitude. After compensating the source voltage, the rectified voltage is delivered to the load. The fault is identified between the time of 0.5 seconds and 0.7 seconds. The amplitude of source voltage has sagged to 4kV, and it is regulated to 11kV after 0.7 seconds. The rectified voltage is given to EAF without any interruptions. Figure 5 describes the effective performance of source voltage and load voltage. The simulation response is obtained for three phases corresponding to the three-phase AC source.

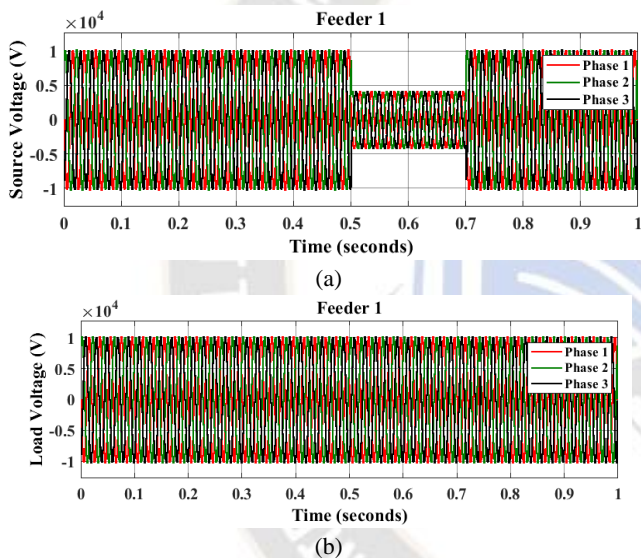


Figure 5: Simulation response of source voltage and load voltage for feeder-1 under the sagging condition

Similarly, the source current for feeder-1 is optimized as 150A, and defects in the source current are analyzed through DSTATCOM. The response was obtained for 1 second, and the fault occurred between 0.5 and 0.7 seconds. During sag fault, the amplitude of a source current sagged to 60A, and it is rectified to reach the amplitude of 150A. Therefore DSTATCOM with FOFPID controller effectively regulates the source current for the load current. Figure 6 illustrates the characteristics response of source current and load current under sag conditions.

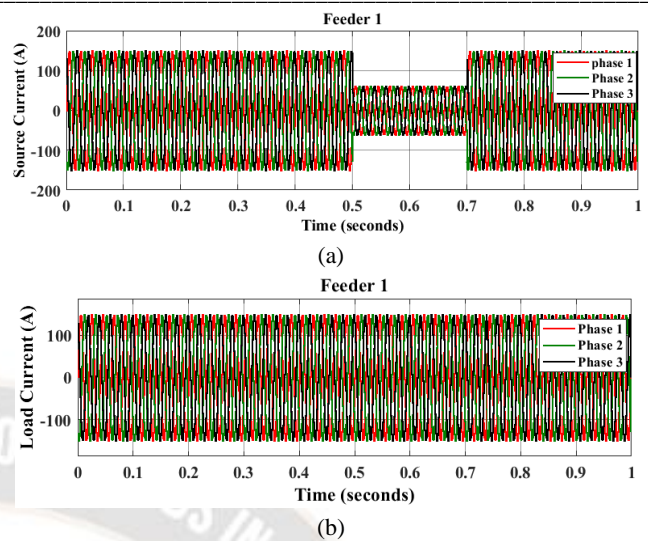


Figure 6: Simulation response of source current and load current for feeder-1 under the sagging condition

The swelling fault in feeder-1 is detected and rectified using FOFPID and DSTATCOM compensator. The amplitude of a source voltage is diagnosed as 11kV over 1 second. The swelling fault occurs between 0.1 and 0.3 seconds with an amplitude of 15kV. This swelled amplitude is regulated by the DSTATCOM by injecting the compensation voltage to the source. Therefore the proposed FOFPID with DSTATCOM compensator effectively restores the load voltage. The regulated supply is delivered to the EAF through the controller and DSTATCOM compensator. The simulation response obtained for source and load voltage under swelling conditions is described in Figure 7.

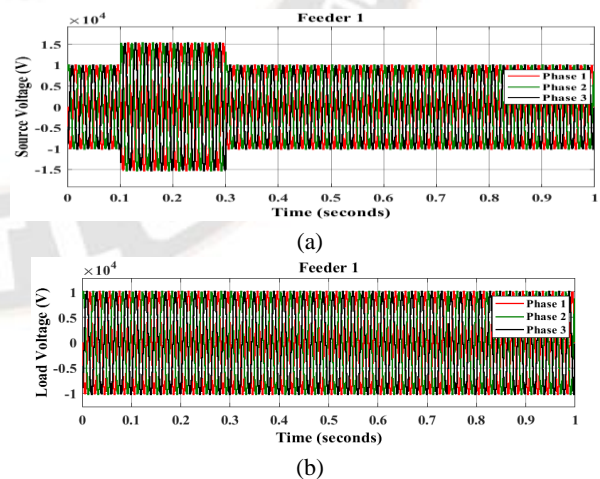


Figure 7: Characteristics response of source voltage and load voltage for feeder-1 under the swelling condition

Likewise, the controller compensates the source current concerning the compensator. The amplitude of a source current is evaluated as 150A, and the swelled current amplitude is considered as 220A. The DSTACOM compensates the source

current based on ICC characteristics and makes the amplitude 150A. Also, the FOFPID controller regulates the source current concerning the demand side and keeps the system stable. Figure 8 signifies the response obtained for load and source current under swelling conditions. Table 5 reveals the voltage and current characteristics in feeder-1.

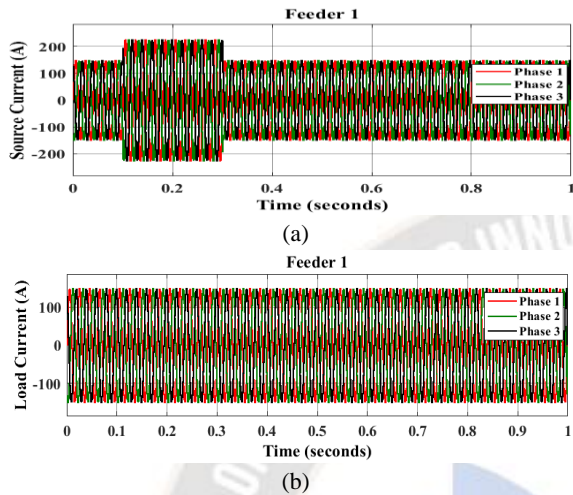


Figure 8: Performance of source current and load current for feeder-1 under the swelling condition

Table 5: Current and voltage characteristics of feeder-1

Components (feeder-1)	Sag		Swell	
	Actual	Sagged	Actual	Swelled
Source voltage (kV)	11	4	11	15
Source current (A)	148	60	148	220
Load voltage (kV)	11		11	
Load current (A)	148		148	

C. Simulation response of feeder-2 for proposed IUPQC with FOFPID controller

As with feeder-1, the voltage-current compensation in feeder-2 is performed through DVR with the FOFPID controller. DVR rectifies the defects in a distributed system by injecting the compensation voltage. The characteristics response under sagging fault and the swelling fault is determined for feeder-2. The NLL is connected to feeder-2, and the performance of a DVR is analyzed through two cases.

The sagging fault rectification is performed for feeder-2 based on DVR and FOFPID controller. The time for determining the characteristics of DVR is assumed to be 1 second. The fault was applied between 0.1 and 0.3 seconds with a sagging amplitude of 4kV. The FOFPID controller regulates the source voltage, and DVR injects the rectified voltage to generate the compensation voltage. Figure 9 depicts the characteristics response of source and load voltage for feeder-2. This regulated voltage is supplied to the NLL through DVR and FOFPID controller.

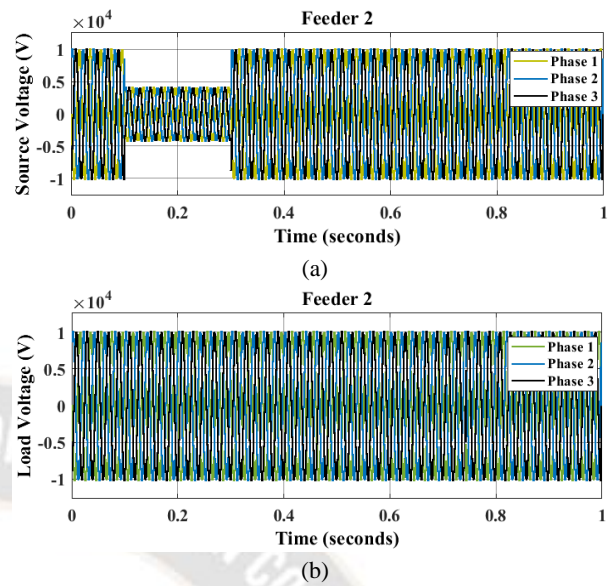


Figure 9: Simulation response of source voltage and load voltage for feeder-2 under the sagging condition

Furthermore, DVR compensates the source current and rectifies the defects in a source current response. The optimum current range for dual feeder construction is -150A to 150A. FOFPID controller detects that the amplitude of a source current sagged to 60A due to the defects in a source current. FOFPID regulates the defective source current, and the DVR compensator injects sufficient current. Therefore, the optimized supply is given to the NLL without any distortions. This characteristic response reveals the effective performance of a proposed converter and compensator. Figure 10 illustrates the source and load current behaviour for feeder-2 under sagging conditions.

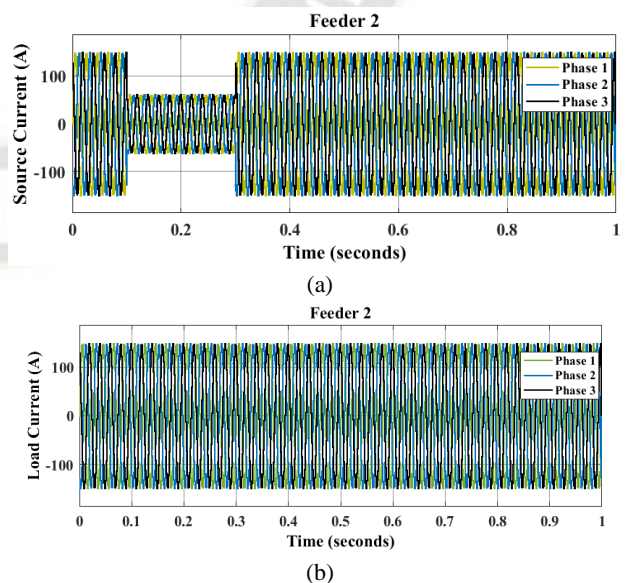


Figure 10: Simulation response of source current and load current for feeder-2 under the sagging condition

The rectification of swelling fault using DVR with FOPID controller is demonstrated effectively. A source voltage's maximum amplitude is assumed to be 11kV, but the voltage gets interrupted with 15kV. FOPID controller regulates the source voltage with interruptions. Also, DVR injects the regulated voltage to the source and generates the compensated voltage with an amplitude of 11kV. The time duration for determining the performance of DVR is considered as 1 second. The three-phase voltage gets distorted during the fault occurs in the source voltage. Figure 11 depicts the effective source and load voltage performance for feeder-2 under swelling conditions.

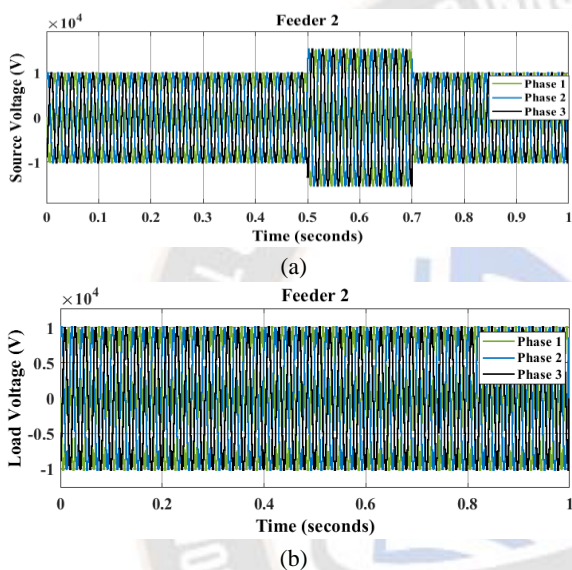


Figure 11: Characteristics response of source voltage and load voltage for feeder-2 under the swelling condition

Consequently, a hybrid renewable source-connected system determines the rectified load current. The hybrid sources generate the source current, and an amplitude reaches the optimum value of 150A. But the distortion is analyzed between the time duration of 0.5 seconds and 0.7 seconds. The defective source current attains the voltage of 220A, and the proposed DVR compensator restores this response. The FOPID controller and DVR compensate the source current and rectify the input defects. Figure 12 represents the source and load current performance for feeder-2 under swelling conditions.

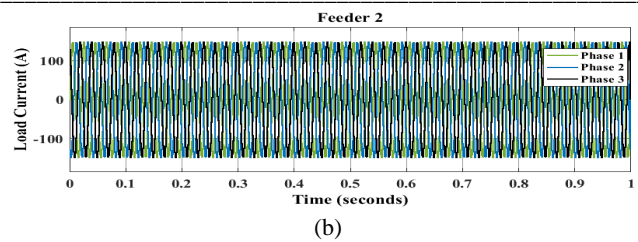
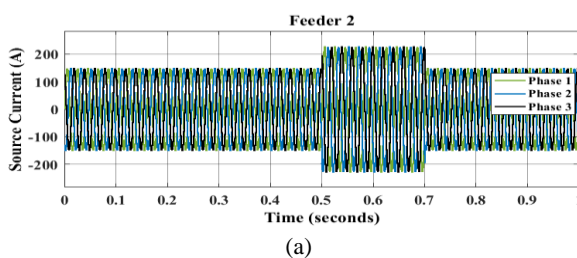


Figure 12: Performance of load current and source current for feeder-2 under the swelling condition

Therefore, the simulation response reveals the functionality of a proposed IUPQC with the FOPID controller. The PQ problems in dual feeders are effectively compensated, and the proposed controller maintains stability in the system. Thus, the supply voltage is regulated effectively without affecting any disturbances in the distributed system. Table 6 describes the response values for voltage and current in feeder-2.

Table 6: Voltage and current characteristics of feeder-2

Components (feeder-2)	Sag		Swell	
	Actual	Sagged	Actual	Swelled
Source voltage (kV)	11	4	11	15
Source current (A)	150	60	150	220
Load voltage (kV)	11		11	
Load current (A)	150		150	

D. Performance of THD for proposed IUPQC with FOPID controller

For verifying the robustness of a proposed IUPQC with FOPID controller, the THD is also analyzed for the source voltage, load voltage, source current and load current. The THD is examined for the dual feeders, and the proposed controller obtained minimum THD. The stability of a system is demonstrated through the behaviour of DSTATCOM and DVR compensators. The compensators effectively provide stability to a system by enhancing the PQ troubles in dual feeders.

1 THD response for feeder-1

For feeder-1, the THD is evaluated for components such as source voltage, load voltage, source current and load current and the achieved results are shown in Figure 13. The THD is diagnosed for about 50Hz, and the response reveals the minimum distortions. The THD for a source current is 2.09%, and the THD for a load current is 1.25%. Similarly, the THD for a source voltage is obtained as 0.13%, and THD for the load voltage is 1.45%. Therefore, the proposed controller regulates the PQ events in dual feeders with fewer distortions.

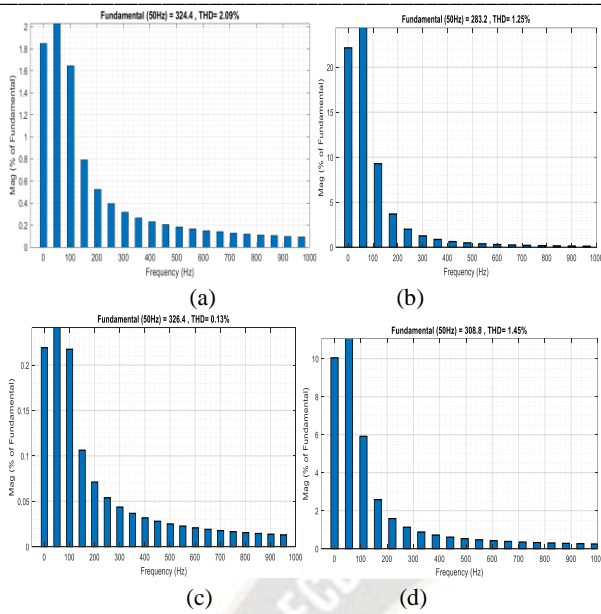


Figure 13: THD response of (a) source current, (b) load current, (c) source voltage and (d) load voltage for feeder-1

2 THD results for feeder-2

The THD characteristics in feeder-2 are analyzed for the feeder components such as source voltage, load voltage, source current and load current and the obtained results are shown in Figure 14. THD is examined over a frequency of about 50Hz, and obtained performance reveals the feasibility of a proposed IUPQC with a FOPPID controller. The THD for a source current is demonstrated as 1.67%, and the THD for a load current is revealed as 1.38%. Likewise, the THD for source voltage is exhibited as 2.3%, and the THD for load voltage is evaluated as 2.5%. This characteristic response shows the efficacy of a proposed IUPQC with a FOPPID controller. Consequently, PQ troubles in the dual feeder are compensated by both DVR and DSTATCOM. Also, the proposed controller maintains stability in a dual-feeder distributed system. Furthermore, the power supply is regulated by a proposed IUPQC with FOPPID controller with fewer distortions.

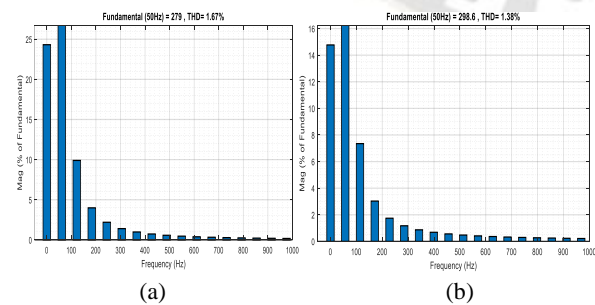


Figure 14: THD performance of (a) source current, (b) load current, (c) source voltage and (d) load voltage for feeder-2

Table 7: Comparative analysis of THD response for proposed and traditional strategies

Parameters	Proposed (FOFPID-IUPQC)		IUPQC-4VSC	
	Feeder-1	Feeder-2	Feeder-1	Feeder-2
Source Current	2.09%	1.67%	3.08%	3.09%
Load Current	1.25%	1.38%	30.84%	30.79%
Source Voltage	0.13%	2.3%	44.72%	25%
Load Voltage	1.45%	2.5%	4.63%	2.59%

The THD response values are compared with the traditional IUPQC-4VSC conditioner, and the proposed controller provides better responses. The comparative analysis of THD for a proposed and traditional methodology is depicted in Table 7. The response reveals the proposed controller enhances PQ with minimum distortions. The existing IUPQC-4VSC conditioner obtained the source current and load current THD of about 3.08% and 30.84% for feeder-1. Similarly, the IUPQC-4VSC conditioner generates the THD for source voltage and load voltage in feeder-1 as 44.72% and 4.63%. The traditional method generates the source current and load current THD for feeder-2 as 3.09% and 30.79%. Likewise, the existing method generates the source voltage and load voltage THD of about 25% and 2.59%. This shows the proposed controller adequately minimizes the THD for both feeders.

V. CONCLUSION

The enhancement of PQ in distributed feeders incorporating hybrid renewable sources is one of the most significant research themes. There are various controllers for improving PQ events in the distributed system. This paper proposes the IUPQC with FOPPID controller for compensating PQ troubles in dual feeders. IUPQC includes both DVR and DSTATCOM compensators for restoring PQ problems in the distributed

system. Moreover, the ICC converter regulates the optimum power flow between DVR and DSTATCOM. DSTATCOM enhances the PQ troubles in feeder-1 by regulating the voltage from a three-phase AC source. Similarly, DVR improves the PQ events in feeder-2 by compensating for the voltage from hybrid renewable sources. The performance of a proposed IUPQC with FOPPID controller is analyzed through MATLAB/Simulink tool. The simulation response reveals the effectiveness of a proposed IUPQC with a FOPPID controller. The effective behaviour of a proposed controller is analyzed through sagging and swelling faults. The faults are exhibited for both feeders, and the corresponding response in the load is determined. Therefore both compensators effectively restore the PQ troubles during dual feeder construction. Furthermore, the robustness of a proposed IUPQC with a FOPPID controller is characterized by finding THD for each parameter. The generated THD results are compared with the traditional IUPQC-4VSC conditioner. For a proposed controller, the THD of source current and load current in feeder-1 is identified as 2.09% and 1.25%. Similarly, the THD of source voltage and load voltage in feeder-1 is obtained as 0.13% and 1.45%. Also, the THD response value of source current and load current in feeder-2 is 1.67% and 1.38%. Likewise, the THD performance value of source voltage and load voltage in feeder-2 is 2.3% and 2.5%. The comparative analysis shows that the THD for a proposed controller is minimized effectively. The overall performance analysis shows that the proposed IUPQC with FOPPID controller is more suitable for enhancing PQ troubles in dual feeders. The characteristic response reveals the efficacy of a proposed controller. The PQ events in the dual feeder will be enhanced in the future using optimized FOPPID controllers.

REFERENCES

- [1] O.P. Mahela, B. Khan, H.H. Alhelou, S. Tanwar and S. Padmanaban, Harmonic mitigation and power quality improvement in utility grid with solar energy penetration using distribution static compensator, *IET Power Electronics* 14(5) (2021) 912-922.
- [2] A.Y. Solanki and S.R. Vyas, Power Quality Enhancement in Distribution System Using D-STATCOM (2021).
- [3] T. Toumi, A. Allali, A. Meftouhi, O. Abdelkhalik, A. Benabdelkader and M. Denai, Robust control of series active power filters for power quality enhancement in distribution grids Simulation and experimental validation, *ISA transactions* 107 (2020) 350-359.
- [4] B. Babes, F. Albalawi, N. Hamouda, S. Kahla and S.M. Ghoneim, Fractional-fuzzy PID control approach of photovoltaic-wire feeder system (PV-WFS) Simulation and HIL-based experimental investigation, *IEEE Access* 9 (2021) 159933-159954.
- [5] V. Verma, R. Singh and R. Gour, ADSIG as Gen-Former providing three port network for soft coupling of distribution feeders in addition to wind energy harvesting, *International Journal of Electrical Power & Energy Systems* 117 (2020) 105573.
- [6] A. Awasthi and V. Rai, Power Quality Improvement Using UPQC with variable DC Link Voltage Control (2020).
- [7] C.R. Reddy, B.S. Goud, F. Aymen, G.S. Rao and E. C. Bortoni, Power quality improvement in HRES grid connected system with FOPID based atom search optimization technique, *Energies* 14(18) (2021) 5812.
- [8] B.S. Goud and B.L. Rao, Power quality improvement in hybrid renewable energy source grid-connected system with grey wolf optimization, *International Journal of Renewable Energy Research (IJRER)* 10(3) (2020) 1264-1276.
- [9] Wanjiku, M., Ben-David, Y., Costa, R., Joo-young, L., & Yamamoto, T. Automated Speech Recognition using Deep Learning Techniques. *Kuwait Journal of Machine Learning*, 1(3). Retrieved from <http://kuwaitjournals.com/index.php/kjml/article/view/135>
- [10] A. Gupta, Power quality evaluation of photovoltaic grid interfaced cascaded H-bridge nine-level multilevel inverter systems using D-STATCOM and UPQC, *Energy* 238 (2022) 121707.
- [11] N.S. Sarita, S.S. Reddy and P. Sujatha, Control strategies for power quality enrichment in Distribution network using UPQC, *Materials Today Proceedings* (2021).
- [12] U.K. Renduchintala, C. Pang, K.M. Tatikonda and L. Yang, ANFIS-fuzzy logic based UPQC in interconnected microgrid distribution systems modeling, simulation and implementation, *The Journal of Engineering* 1 (2021): 6-18.
- [13] C. Kumar, S. Pragaspathy, V. Karthikeyan, and K.D. Prakash, Power quality improvement for a hybrid renewable farm using UPQC, In 2021 International Conference on Artificial Intelligence and Smart Systems (ICAIS) (2021) 1483-1488.
- [14] A.Y. Qasim, F.R. Tahir and A.B. Alsammak, Voltage Sag, Voltage Swell and Harmonics Reduction Using Unified Power Quality Conditioner (UPQC) Under Non-linear Loads, *Iraqi Journal for Electrical & Electronic Engineering* 17(2) (2021).
- [15] P.S. Kumar, Applications of Hybrid Wind Solar Battery Based Microgrid for Small-Scale Stand-Alone Systems and Grid Integration for Multi-Feeder Systems, *Electrical and Electronic Devices, Circuits, and Materials: Technological Challenges and Solutions* (2021) 517-533.
- [16] Prof. Parvaneh Basaligheh. (2017). Design and Implementation of High Speed Vedic Multiplier in SPARTAN 3 FPGA Device. *International Journal of New Practices in Management and Engineering*, 6(01), 14 - 19. Retrieved from <http://ijnpme.org/index.php/IJNPME/article/view/51>
- [17] U. Musa, A.A. Mati, A. Mohammed and A.A. Mas'ud, Implementation of Bacterial Foraging Algorithm Based Model for UPQC Placement in a Practical Distribution Feeder, *COVENANT JOURNAL OF ENGINEERING TECHNOLOGY* 4(1) (2020).
- [18] S.R. Das, D.P. Mishra, P.K. Ray, S.R. Salkuti and A.K. Sahoo, Power quality improvement using fuzzy logic-based compensation in a hybrid power system, *International Journal of Power Electronics and Drive Systems* 12(1) (2021) 576.

- [19] N. Abas, S. Dilshad, A. Khalid, M.S. Saleem and N. Khan, Power quality improvement using dynamic voltage restorer, *IEEE Access* 8 (2020) 164325-164339.
- [20] R.P. Naidu and S. Meikandasivam, Power quality enhancement in a grid-connected hybrid system with coordinated PQ theory & fractional order PID controller in DPFC, *Sustainable Energy, Grids and Networks* 21 (2020) 100317.
- [21] Ahmed Ali, Anaïs Dupont, Deep Generative Models for Image Synthesis and Style Transfer, *Machine Learning Applications Conference Proceedings*, Vol 2 2022.
- [22] B.S. Goud, C.R. Reddy, M. Bajaj, E.E. Elattar and S. Kamel, Power Quality Improvement Using Distributed Power Flow Controller with BWO-Based FOPID Controller, *Sustainability* 13(20) (2021) 11194.
- [23] K. Muthuvel and M. Vijayakumar, Solar PV sustained quasi Z-source network-based unified power quality conditioner for enhancement of power quality, *Energies* 13 (10) (2020) 2657.
- [24] T.S. Prakash, P. S. Kumar and R. P. S. Chandrasena, A Novel IUPQC for Multi-Feeder Systems Using Multilevel Converters with Grid Integration of Hybrid Renewable Energy System, *IEEE Access* 8 (2020) 44903-44912.
- [25] Viswanathan, D., Kumari, S., & Navaneetham, P. (2023). Soft C-means Multi objective Metaheuristic Dragonfly Optimization for Cluster Head Selection in WSN. *International Journal of Intelligent Systems and Applications in Engineering*, 11(2s), 88–95. Retrieved from <https://ijisae.org/index.php/IJISAE/article/view/2513>
- [26] M. Golla, S. Sankar and K. Chandrasekaran, Renewable integrated UAPF fed microgrid system for power quality enhancement and effective power flow management, *International Journal of Electrical Power & Energy Systems* 133 (2021) 107301.
- [27] A. Gowrishankar and M. Ramasamy, SPV-based UPQC with modified power angle control scheme for the enhancement of power quality, *Journal of Circuits, Systems and Computers* 29(4) (2020) 2050064.
- [28] Samad, A. . (2022). Internet of Things Integrated with Blockchain and Artificial Intelligence in Healthcare System. *Research Journal of Computer Systems and Engineering*, 3(1), 01–06. Retrieved from <https://technicaljournals.org/RJCSE/index.php/journal/article/view/34>
- [29] A. Ortega, J.P. Tomy, J. Shek, S. Paboeuf and D. Ingram, An Inter-Comparison of Dynamic, Fully Coupled, Electro-Mechanical, Models of Tidal Turbines, *Energies* 13(20) (2020) 5389.
- [30] P.B. Neto, O.R. Saavedra and D. Q. Oliveira, The effect of complementarity between solar, wind and tidal energy in isolated hybrid microgrids, *Renewable Energy* 147 (2020) 339-355.
- [31] A.A. Imam, R.S. Kumar and Y.A. Al-Turki, Modeling and simulation of a PI controlled shunt active power filter for power quality enhancement based on PQ theory, *Electronics* 9(4) (2020) 637.
- [32] W. Rohouma, R.S. Balog, A.A. Peerzada and M.M. Begovic, D-STATCOM for harmonic mitigation in low voltage distribution network with high penetration of non-linear loads, *Renewable Energy* 145 (2020) 1449-1464.
- [33] B.S. Jebaraj, J. Bennet, R. Kannadasan, M. H. Alsharif, M. Kim, A.A. Aly and M.H. Ahmed, Power quality enhancement in electric arc furnace using matrix converter and static var compensator, *Electronics* 10(9) (2021) 1125.
- [34] K.D. Joseph, A.Z. Daniel and A. Unnikrishnan, Modified Interleaved Cuk Converter with Improved Voltage Gain and Reduced THD, *Arabian Journal for Science and Engineering* (2022) 1-11.
- [35] O. Karahan, Design of optimal fractional order fuzzy PID controller based on cuckoo search algorithm for core power control in molten salt reactors, *Progress in Nuclear Energy* 139 (2021) 103868.